Stochastic sub-grid scale acceleration model (SSAM) for LES of primary atomization using VOF method for ECN Spray-A

Surya Kaundinya Oruganti[1,2] and Mikhael Gorokhovski*[1]
[1]Laboratoire de Mécanique des Fluide et d'Acoustique, Ecole Centrale de Lyon 36, Avenue Guy de Collongue, 69134 Écully Cedex, France
[2]Volvo Group Trucks Technology, 99 Route de Lyon – 69806 Saint Priest Cedex, France
*Corresponding author email: mikhael.gorokhovski@ec-lyon.fr

Abstract
Primary atomization at high Weber numbers evolves in highly sheared gas flow. The latter is characterized by energetic intermittent turbulent structures on small length-scales. Although the effects of turbulent flow dynamics on small scales may strongly correlate with wrinkling of the liquid/gas interface, the residual scales are usually discarded in reduced simulations. In this paper, we present the large eddy simulation (LES) of primary atomization of a diesel spray jet using VOF method accounting for intermittency effects on sub-grid scale liquid/gas interface. The principal idea of this approach is to force the filtered Navier Stokes equation by the subgrid acceleration, which is modelled in a way to represent the main statistical properties of intermittency in the high Reynolds number flows. Earlier, this approach was referred to as LES-SSAM (stochastic subgrid acceleration model). In this approach, the statistics of acceleration on residual scales is modelled by two independent stochastic processes i.e., one for the norm and the other for the unit orientation vector. The both are modelled by Ornstein-Uhlenbeck process: while the norm is modelled by a long-correlated log-normal process, the acceleration orientation vector is modelled by diffusion on the unit sphere with relaxation towards the local vorticity field, and with correlation on the short Kolmogorov time. The resulting stochastic velocity field is then used for reconstruction of the liquid/gas interface in the framework of iso-advector geometrical VOF method. The approach is applied to simulate the primary atomization of ECN Spray-A injector. A qualitative comparison of liquid/gas interface evolution with the under-resolved LES-VOF approach is provided.

Keywords
Spray breakup, stochastic, log-normal process, viscous dissipation rate and ECN Spray-A.

Introduction

A liquid jet issued from a typical high pressure diesel injector is highly sheared by the in-nozzle flow phenomenon like turbulence and cavitation, which significantly affect the evolution of the spray and subsequent fuel-air mixing [1-3]. The largely used Euler-Lagrangian approach for modeling of atomization using computational droplets in conjunction with phenomenological breakup models do not provide detailed information on effects of in-nozzle flow conditions on liquid jet evolution. To this end over the past two decades, several single fluid Eulerian modelling approaches based on construction of liquid/gas interface and tracking its evolution at each time step like the front tracking method [4], level-set [5] and volume of fluid or VOF [6] have been developed. While several DNS studies have shown the efficiency of these approaches in modelling of high-speed liquid jet atomization, they are computationally very expensive. On the other hand, in Large Eddy Simulation (LES) of atomization using these interface capturing approaches, it is a common practice to overlook the small-scale turbulence effects on the sub-grid wrinkling of liquid/gas interface. However recent studies of [7] have shown that interaction of the residual scale turbulence structures on sub-grid liquid/gas interface dynamics is significant and requires modelling. To address this issue, [8] formulated

a dual-scale approach to model the sub-grid scale (SGS) liquid/gas interface dynamics. The idea was to obtain a fully resolved interface geometry by modelling SGS velocity required to transport the interface on an auxiliary grid using refined level set method. Based on similar principles, in this paper an attempt is made to present the LES of primary atomization of a diesel spray jet using VOF method accounting for intermittency effects on sub-grid scale liquid/gas interface dynamics. The principal idea is to obtain a full realization of the velocity field by forcing the filtered Navier Stokes equation by the subgrid acceleration, which is modelled in a way to represent the main statistical properties of intermittency in the high Reynolds number flows as outlined in [9-11]. This approach is referred to as LES-SSAM (stochastic sub-grid scale method). The surrogate velocity field realized from solution of stochastic Navier Stokes equation, is then used for reconstruction of the liquid/gas interface using the iso-advector geometrical VOF method of [12].

In the following sections, first a detailed description of the governing equations for the volume of fluid (VOF) approach, filtered LES-VOF and LES-SSAM are provided. This is followed by a description of the iso-advector VOF approach. Next a qualitative assessment of LES-SSAM approach for primary atomization of liquid jet with conditions corresponding to ECN Spray-A experiment are provided.

LES-VOF Governing Equations

The atomization process is usually modelled using unsteady incompressible Navier Stokes Equations assuming the liquid-gas system as a single fluid with variable density as given by Eq. (1-2).

$$\nabla . \mathrm{u} = 0 \tag{1}$$

$$\frac{\partial \rho \mathrm{u}}{\partial \mathrm{t}} + \mathrm{u} . \nabla \rho \mathrm{u} = -\nabla . \mathrm{p} + \nabla . (\rho \nu (\nabla \mathrm{u} + \nabla u^{\mathrm{T}})) + \mathrm{T}_{\sigma} \tag{2}$$

where u is the velocity, p is the pressure, ρ is the spatially varying density, ν is the kinematic viscosity of liquid-gas system. The term T_{σ} represents the surface tension force acting only at the liquid-gas interface. The liquid-gas interface is represented by a material surface whose motion is described by the transport equation of the liquid volume fraction field α.

$$\frac{\partial \alpha}{\partial \mathrm{t}} + \mathrm{u} . \nabla \alpha \ = 0 \tag{3}$$

The liquid volume fraction α is the spatial average of the phase indicator function *H(x,t)* in each computational cell Ω with volume *V*.

$$\alpha \ = \frac{\mathbf{1}}{\boldsymbol{V}} \int_{\Omega} H(x,t) dx \tag{4}$$

$$H(x,t) = \begin{cases} 0 & \text{if x is in the gas} \\ 1 & \text{if x is in the liquid} \end{cases} \tag{5}$$

Assuming the density and viscosity of the two fluids to be constants, the spatially varying fluid properties of the liquid-gas system are expressed as volume average of the fluids.

$$\rho \ = \ \alpha \, \rho_{\mathrm{l}} \ + (1 - \alpha) \, \rho_{\mathrm{g}} \tag{6}$$

$$\nu \ = \ \alpha \, \nu_{\mathrm{l}} \ + (1 - \alpha) \, \nu_{\mathrm{g}} \tag{7}$$

And the surface tension force at the liquid-gas interface is given by the widely used the continuum surface force method [13].

$$\mathrm{T}_{\sigma} \ = \ \sigma \kappa \, \nabla \alpha \tag{8}$$

where σ is the surface tension coefficient and κ is the mean interface surface curvature.

In case of LES, the instantaneous flow field variable f, is usually decomposed into a filtered ($\bar{f}$) and SGS components (f').

$$f = \bar{f} + f' \tag{9}$$

The filtered Navier Stokes equations and the liquid volume fraction transport equation are given by Eq. (10-11).

$$\frac{\partial \overline{\rho \mathrm{u}}}{\partial \mathrm{t}} + \bar{\mathrm{u}}\nabla.\overline{\rho \mathrm{u}} = -\nabla.\bar{\mathrm{p}} - \nabla(\nabla.(\rho(\nu + \nu_{sgs})\left(\nabla\bar{\mathrm{u}} + \nabla\bar{\mathrm{u}}^{\mathrm{T}}\right)) + \overline{\mathrm{T}_{\sigma}} + \mathrm{T}_{\sigma,\mathrm{sgs}} \tag{10}$$

$$\frac{\partial \bar{\alpha}}{\partial \mathrm{t}} + \bar{\mathrm{u}}.\nabla\bar{\alpha} + \nabla.\overline{\mathrm{u}'\alpha'} = 0 \tag{11}$$

In this study, the one-equation eddy viscosity model [14] is used, where SGS viscosity is calculated from the subgrid kinetic energy (k_{sgs}) and the filter width (Δ) i.e., $\nu_{sgs} = C_k\Delta\sqrt{k_{sgs}}$. The solution for the SGS kinetic energy k_{sgs} is obtained from a transport equation accounting for its production, dissipation and convection as outlined in [14]. In the above system of filtered equations in addition to the SGS turbulent viscosity ν_{sgs}, two more terms require closure i.e., the SGS surface tension forces $\mathrm{T}_{\sigma,\mathrm{sgs}}$ and the term $\mathrm{u}'\alpha'$, correlating the SGS velocity fluctuations with the SGS wrinkling of the liquid/gas interface. However, in common practice these terms are neglected resulting in an under-resolved LES-VOF solution.

LES-SSAM – Stochastic SGS Acceleration Model

Based on the works of [9-11], in this study we attempt to account for the intermittency effects of residual scale turbulence on the SGS interface dynamics by providing in the filtered momentum equation an access to the fluid acceleration on residual scales a_{sgs} as shown in Eq. (11).

$$\frac{\partial \overline{\rho \mathrm{u}}}{\partial \mathrm{t}} + \bar{\mathrm{u}}\nabla.\overline{\rho \mathrm{u}} = -\nabla.\bar{\mathrm{p}} - \nabla(\nabla.(\bar{\rho}(\nu + \nu_{\mathrm{sgs}})\left(\nabla\bar{\mathrm{u}} + \nabla\bar{\mathrm{u}}^{\mathrm{T}}\right)) + \overline{\mathrm{T}_{\sigma}} + \bar{\rho}a_{sgs} \tag{11}$$

The solution of the stochastic Navier Stokes equation obtained from Eq. (11) gives a surrogate velocity field which accounts for the intermittency effects of residual scales and is different from the classical LES approach. Based on experimental observations [14-16] of the fluid particle acceleration, it was proposed by [9] to model the SGS acceleration term using two independent stochastic processes i.e., the norm of the acceleration with long-term correlation characterized by integral time scales and the unit orientation vector of acceleration fluctuating on short time scales corresponding to Kolmogorov time scale.

$$a_{sgs} = |a|(t)e_i(t); \; e_i e_i = 1 \tag{12}$$

The norm of the SGS acceleration is modelled using a log-normal process given by Eq. (13) and is derived from Ito-transformation of the log-normal process for dissipation rate of [17]. In Eq. (13) while the dispersion term σ^2 is modelled as a function of the local flow Reynolds number, the correlation time T is given by the integral time scale as shown in Eq. (14).

$$d|a| = -|a|\left(ln\left(\frac{|a|}{a_\eta}\right) - \frac{3}{16}\sigma^2\right)\frac{dt}{T} + \frac{3}{4}|a|\sqrt{\frac{2\sigma^2}{T}}dW(t) \tag{13}$$

$$\sigma^2 = \ln\frac{\Delta}{\eta}; \; \mathrm{T}^{-1} = \frac{\nu_{\mathrm{t}}}{\Delta^2} \tag{14}$$

where $a_\eta = (\varepsilon^3/\nu_{\mathrm{t}})^{\frac{1}{4}}$ is the fluid acceleration on Kolmogorov length scales and $dW(t)$, is the increment of a standard Brownian process,$\langle dW\rangle$=0, $\langle dW^2\rangle$=*dt*. Next the orientation of the SGS unit directional vector at each spatial point is emulated by Ornstein-Ulhenbeck (OU) process on unit sphere with relaxation towards local vorticity field as outlined in [10].

$$de_i = -h_{\perp,i} T_{rel}^{-1} dt + \left(\delta_{ij} - e_i e_j\right) \sqrt{2 T_{diff}^{-1}} dW_{xj} \quad (15)$$

In Eq. (15) the first term represents the stochastic relaxation towards a presumed direction with its components h_i and its projection form $h_{\perp,i} = h_i - \left(h_j e_j\right) e_i$. The presumed direction vector h is given by the unit vector $e_{\omega,i} = \frac{\omega_i}{|\omega|}$, where ω_i are the components of local resolved vorticity field. Next in Eq. (15) while $T_{rel} = {k_{sgs}}/{\varepsilon}$ is the relaxation time, T_{diff} is the diffusion time represented by the Kolmogorov time scale τ_η giving a short-time correlation for the fluctuations of the orientation vector. Earlier assessments of this approach [9,11] with DNS statistics of fluid particle acceleration in HIT and homogenously sheared turbulence has shown the ability to accurately predict the non-gaussian statistics of acceleration on relatively coarse grids compared to classical LES. The surrogate velocity field obtained from solution of Eq. (11) is then used to solve the transport equation of the liquid volume fraction.

Iso-advector VOF method

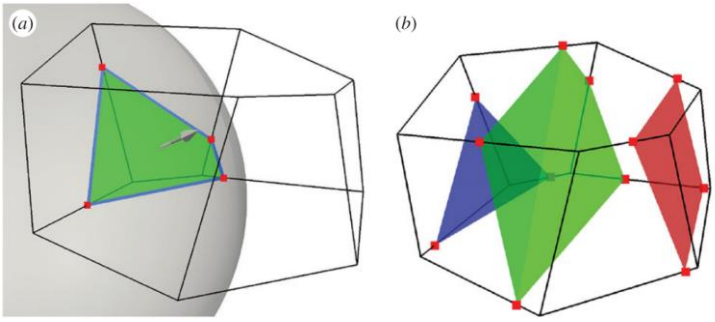

Figure 1. A spherical surface cutting a polyhedral cell. Red dots are the edge cutting points. Blue lines are the face-interface intersection lines. Green patch is the isoface. (b) The isoface motion is estimated from the surrounding velocity data and the isoface is propagated. Isoface at three different times within a time step are shown. Sourced from [12].

Over the past two decades, several VOF methods have been developed for advection of the interface conserving mass and ensuring a sharp-interface. Based on [17] the VOF schemes are broadly classified into *algebraic* methods which are diffusive in nature resulting a smeared interface and *geometric* methods which are more accurate but computationally intensive to implement on complex unstructured grids. However, in recent times, [12] proposed an efficient geometric VOF scheme referred to as *isoAdvector* method which is computationally less intensive while retaining high accuracy of other geometric VOF methods. The efficacy of this approach in simulating a diesel spray atomization using high Courant numbers has been reported in [18]. Therefore, in this study the *isoAdvector* method is used in conjunction with the LES-SSAM approach. In this section the basic idea and the algorithm of *isoAdvector* scheme as presented in [12] is revisited breifly. Let us considered a geometrical domain discretized with a large number of control volumes or cells C_i, $i = 1,2,3,\ldots,N$. The shared surface between any two adjacent control volumes *i* and *j* is referred to as a face and is donated by F_j. The discretized form of the transport equation for the liquid volume fraction over a control volume *i* with volume V_i is given by Eq. (16).

$$\alpha_i(t + \Delta t) = \alpha_i(t) - \frac{1}{V_i} \sum_f \Delta V_f(t, \Delta t) \quad (16)$$

$$\Delta V_j(t, \Delta t) = \int_t^{t+\Delta t} \int_j H(x,\tau) u(x,\tau) \,.\, dS d\tau \quad (17)$$

where $\Delta V_j(t,\Delta t)$ is the volume of liquid transport in/out of control volume *i* from a face F_j shared with its neighbouring control volume *j.* The summation provides the total liquid volume entering a given cell from all the faces shared with its neighbouring cells in the time interval of $(t, t+\Delta t)$. Assuming the velocity field is constant during Δt and approximating the scalar product of velocity $u(x,t)$ and surface normal dS in terms of the volumetric flux across the face F_j i.e., $\phi_f(x,t)$ the Eq. (16) can be further simplified in terms of Eq. (18).

$$\Delta V_j(t,\Delta t) \approx \frac{\phi_j}{|S|}\int_t^{t+\Delta t}\int_j H(x,\tau)\, dSd\tau \;=\; \frac{\phi_j}{|S|}\int_t^{t+\Delta t} A_j(\tau)d\tau \tag{18}$$

where $|S|$ is the surface area of the face F_j and $A_j(t) = \int_j H(x,\tau)\, dSd\tau$ is the instantaneous area of F_j submerged in liquid This reduces the problem of constructing an efficient VOF scheme to calculating the time evolution and subsequently the integral of the area submerged in the liquid $A_j(t)$ for all the faces of a control volume over a given time step. In *isoAdvection*, the starting point for calculating $A_j(t)$ is the construction of a *isoface* in cell upwind of face F_j from which there is an influx of liquid during the time interval $(t, t+\Delta t)$. An *isoface* is a planar surface with an iso-value f which cuts a given control volume into sub-volumes with correct volumetric proportion of liquid and gas phase depending on the liquid fraction α_i as shown in **Figure 1(a)**. It is constructed by interpolating the volume fraction from centres of control cell volumes to the grid points of the discretized mesh using the inverse of distances between the cell centres and the grid points as weights. Let us denote the vertices of a cell *i* by $X_1, X_2, X_3 \ldots\ldots X_N$ and the corresponding interpolated volume fractions at these vertices to be $f_1, f_2, f_3 \ldots\ldots f_N$. Now for each cell edge (X_k, X_l), if the values $f_k < f < f_l$ the edge is cut at point x_{cut} as given by Eq. (19). All these edges obtained for a control volume *i* when connected across faces form the face-interface intersection lines, which when connected together give the *isoface* as shown in **Figure 1(a)**.

$$x_{cut} = X_k + \frac{f-f_k}{f_k-f_l}(X_k - X_l) \tag{19}$$

The isoface splits the control volume into a polyhedral cell, $A_i(f)$, entirely in liquid, and another cell, $B_i(f)$, entirely in gas. The correct iso-value f is recovered by equating the geometrically obtained volume fraction of polyhedral cell $A_i(f)$ to the cell volume fraction as shown in Eq. (20).

$$\tilde{\alpha}(f) \;=\; \frac{vol(A_i(f))}{V_i} \;\approx\; \alpha_i \tag{20}$$

Once the isoface is constructed from the solution of Eq. (20) then the isoface velocity normal to itself U_s in a given time step has to be calculated. This is obtained by interpolating the velocity data from the cell vertices to the centre of isoface x_s and then taking its scalar product with $\hat{n}_s$ the unit normal vector of isoface. The motion of the isoface is shown in **Figure 1(b)**. With the knowledge of x_s, U_s and $\hat{n}_s$ the next step is to calculate the time evolution of face-interface intersection lines for each face F_j. For this first we need to calculate the times at which the isoface travelling at speed U_s normal to itself will reach each of the vertex points of face F_j. Let us assume the vertices of a face F_j be $X_1, X_2, X_3 \ldots\ldots X_N$ and the corresponding times at which iso-faces passes these points to be $t_1, t_2, t_3 \ldots\ldots t_N$. Then these times can be estimated by Eq. (21) and the face-interface intersection lines at these times are schematically shown in **Figure 2(a)**.

$$t_k = t + \frac{\hat{n}_s}{U_s}.(X_k - x_S) \quad \text{for k=1 to N} \tag{21}$$

As shown in **Figure 2(b)** assuming that AB denotes the line segment at time t_k and CD denotes the line segment at time t_{k+1}, then for a time $\tau \in (t_k, t_{k+1})$ the end points of the face-interface intersection are given by points.

$$\tilde{C}(\tau) = B + \frac{\tau - t_k}{t_{k+1} - t_k}(C - B);\ \tilde{D}(\tau) = A + \frac{\tau - t_k}{t_{k+1} - t_k}(A - D) \tag{22}$$

To calculate the time integral of the submerged area, $A_j(t)$ in Eq. (18), we first generate a sorted list of times $\tilde{t}_1, \tilde{t}_2, \tilde{t}_3 \ldots\ldots \tilde{t}_M$, starting with $\tilde{t}_1 = t$, and ending with $\tilde{t}_M = t + \Delta t$, and with a sorted list of all the $t_k's$ from Eq. (21) satisfying $t < t_k < t + \Delta t$. Then the time integral in Eq. (18) can be split up as summation of integrals over these time intervals as shown in Eq. (22).

$$\int_t^{t+\Delta t} A_j(\tau) d\tau \ = \ \sum_{k=1}^{M-1} \int_{\tilde{t}_k}^{\tilde{t}_{k+1}} A_j(\tau) d\tau \tag{22}$$

On each of these sub-intervals, the face-interface intersection line sweeps a quadrilateral as shown in Figure 2b. Using the definitions provided by Eq. (21) the area submerged at any intermediate time $\tilde{t}_k < \tau < \tilde{t}_{k+1}$ can be expressed by functional form shown in Eq. (23) with the coefficients P_k, Q_k calculated analytically from $A, B, \tilde{C}$ and $\tilde{D}$.

$$A_j(\tau) = A_j(\tilde{t}_k) + \frac{1}{2} sign(U_s) \left| A\tilde{C} \times B\tilde{D} \right| = P_k \tau^2 + Q_k \tau + A_j(\tilde{t}_k) \tag{23}$$

The sign of U_s determines if the control volume is gaining or losing fluid A during the time interval. Subsequently the time-integral for sub-interval $(\tilde{t}_k, \tilde{t}_{k+1})$ reduces to,

$$\int_{\tilde{t}_k}^{\tilde{t}_{k+1}} A_j(\tau) d\tau \ = \frac{1}{3}[\tilde{t}^3{}_{k+1} - \tilde{t}^3{}_k\ ]\ P_k + \frac{1}{3}[\tilde{t}^2{}_{k+1} - \tilde{t}^2{}_k\ ] Q_k + [\tilde{t}_{k+1} - \tilde{t}_k\ ] A_j(\tilde{t}_k) \tag{24}$$

From the time-integration of all sub-intervals we can analytically calculate the $\Delta V_j(t, \Delta t)$ and with summation of $\Delta V_j(t, \Delta t)$ over all faces we can update the liquid volume fraction $\alpha_i(t + \Delta t)$ in cell. The final step involves the redistribution of $\Delta V_j(t, \Delta t)$ over the faces and recalculation of $\alpha_i(t + \Delta t)$ for the cells with $\alpha_i(t + \Delta t) < 0$ and $\alpha_i(t + \Delta t) > 0$ to ensure boundedness before proceeding to the next time step.

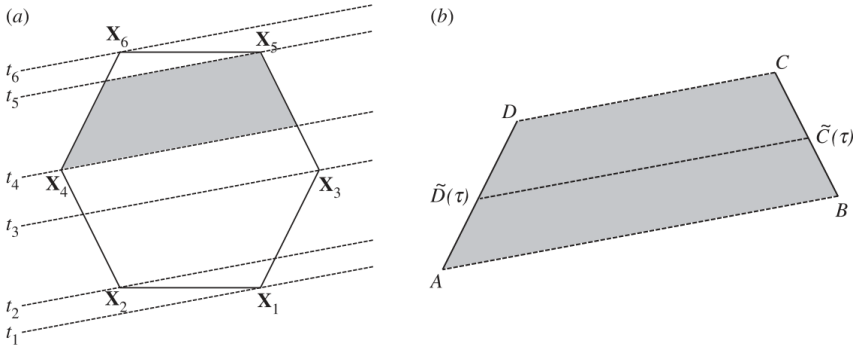

Figure 2. Evolving face-interface intersection line drawn for each time it passes a vertex (dashed lines). An example of the area swept between two such times is marked (grey quadrilateral). (b) Auxiliary notation for calculation of face-interface intersection line at intermediate times.

Liquid jet atomization – ECN Spray-A

A representative geometry of *a* standardised injector geometry with a nozzle diameter of 90 µm referred to as *Spray-A* is used to simulate the in-nozzle flow turbulence. The injector geometry is reconstructed by X-ray tomography and optical microscopy [19-21] and is widely used with the *Engine Combustion Network (or ECN)* community to characterize near-nozzle spray evolution in terms of liquid volume fraction statistics. The *n-dodecane* fuel jet with a

constant density of 715 kg/m^3 is issued at an injection pressure of 150MPa into a constant volume spray chamber filled with an ambient gas at a pressure of 2MPa. Using liquid density, injection and ambient pressures and the nozzle outlet diameter, the bulk flow velocity at the nozzle exit can be estimated to be around 600m/s using Bernoulli's formula. From the nozzle exit velocity and the nozzle outlet diameter the flow Reynolds number is expected to be around $\mathbf{5.4 \times 10^4}$. For simulating the near-nozzle spray atomization process a cylindrical domain of radius 1.6mm and a length of 16 mm is used. Taking the nozzle diameter to be the characteristic length scale (i.e., *L= 90 μm*), the Kolmogorov length scale $\left(\eta = LRe^{-3/4} < 0.1\mu\text{m}\right)$ is in the sub-micron range and is computationally very expensive to resolve. Therefore, in this study we used a non-uniformly discretized mesh with cell sizes varying from 2μm in the near-nozzle region to 16μm near the exit of the computational domain. A first order *Euler* time integration scheme is used along with second order *vanLeer* scheme for spatial discretization of the flux terms. Assuming the needle position is fixed at the opening condition, the nozzle exit velocities from a priori nozzle flow simulation are sampled once in every 10ns for over a period of 100μs. The sampled velocity profiles are imposed as inlet velocity boundary condition for the VOF calculations. Two computations are performed one with *standard LES* (i.e., without any sub-grid scale models) and the other with *LES-SSAM* using isoAdvector VOF method for a duration of 100 μs. The maximum Courant number which determines the maximum time step value is assumed to be 0.5. A comparison of the mean liquid volume fraction statistics at different cross-sections predicted by the two approaches is shown in **Figure-3**. The statistics are obtained from time-averaging over a period of 50 μs.

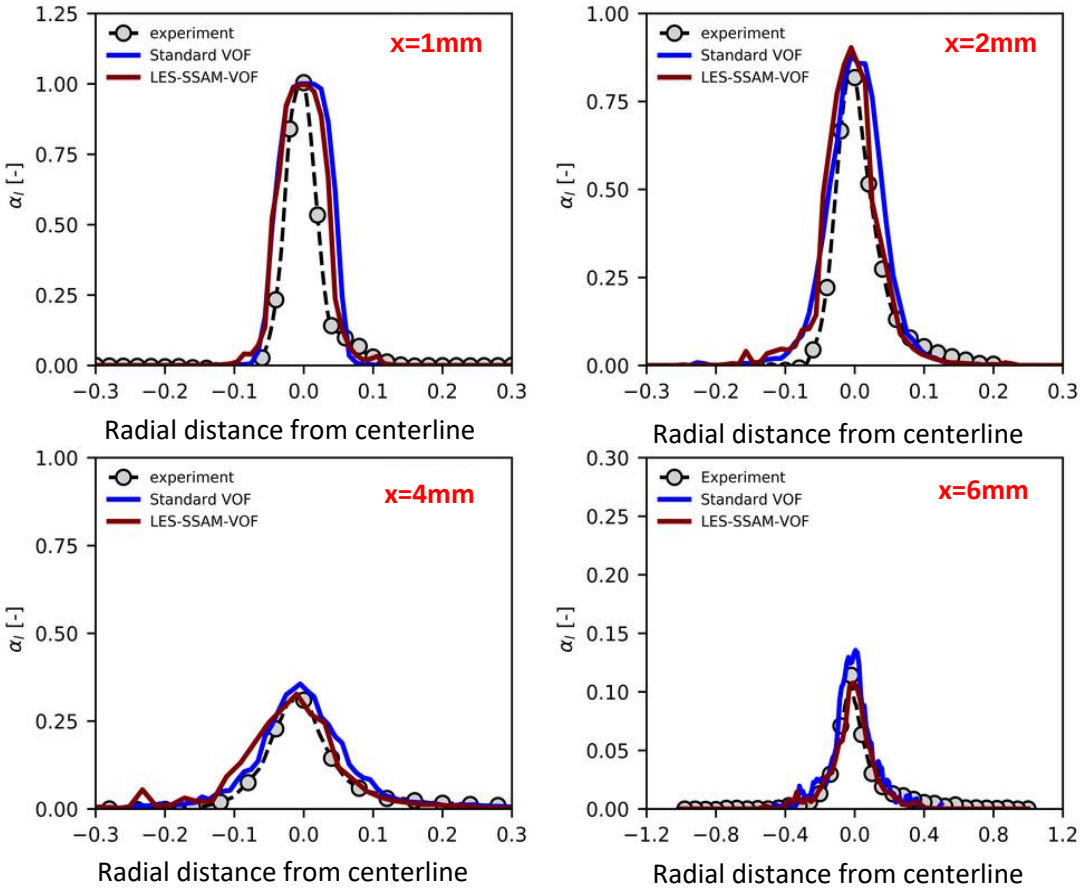

Figure 4. Comparison of time averaged mean liquid volume fraction profiles obtained from *standard LES* and *LES-SSAM* approaches with the experimental results [20] along radial cross sections at axial distances of x=1mm, 2mm, 4mm and 6mm.

It can be seen that both the approaches accurately predict the mean statistics fairly well. Even though both the approaches predict similar first-order statistics of liquid volume fraction, a comparison of the temporal evolution of the liquid jet expressed in terms of *iso-surface* of liquid volume fraction α_l*=0.5* show that with the *LES-SSAM* approach the jet-surface instabilities are initiated much closer to the nozzle exit resulting in shearing of larger number of smaller ligament structures downstream compared to the *standard LES*. The temporal evolution of the *iso-surface* of liquid volume fraction α_l*=0.5* for four different time instances *t=1,2,4* and *8 µs* predicted by *LES-SSAM* (on left) and *standard LES* (on right) is shown in **Figure-4**.

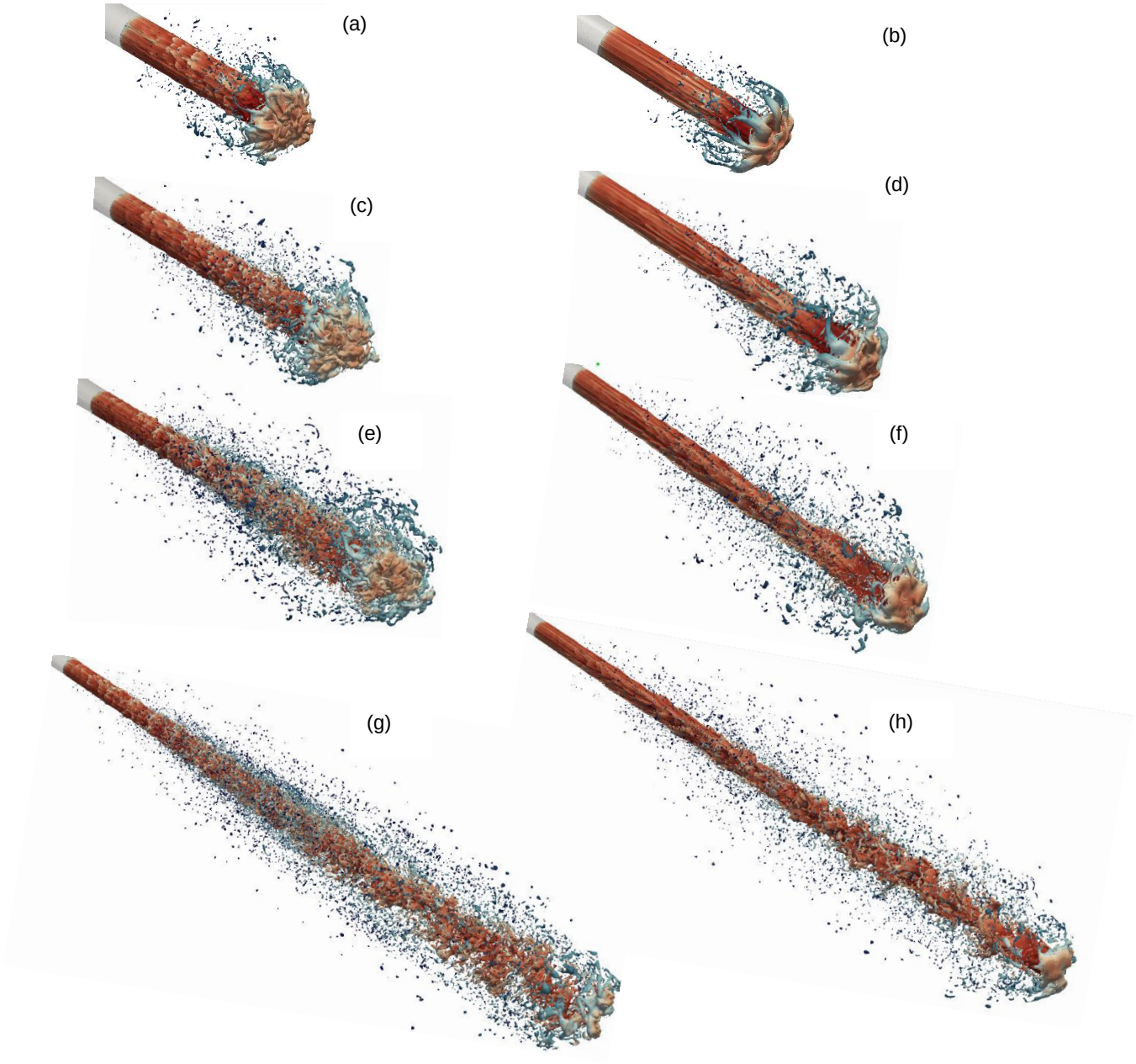

Figure 4. Iso-surface of liquid volume fraction $\alpha_l = 0.5$ for time instances t=1,2 4 and 8 µs. The liquid jet structure predicted by LES-SSAM for the corresponding time instances are shown in figures - (a), (c), (e) and (g) on the left-hand side. Similarly, the liquid jet structure predicted by standard LES-VOF method are shown in figures – (b), (d), (f) and (h) on the right.

Conclusions

In this paper a new stochastic approach has been presented for simulating the sub-grid scale dynamics of liquid-gas interface in LES of high-speed liquid jet atomization using VOF approach. The principal idea is to obtain a surrogate velocity field representing the fully resolved turbulent flow by forcing the sub-grid scale acceleration term onto the filtered momentum equation. The statistics of sub-grid scale acceleration are modelled using two independent stochastic processes i.e., log-normal process for the norm of the acceleration and Ornstien-Ulhenbeck process for the random orientation of the unit vector of acceleration. With the knowledge of the surrogate velocity field the interface is then re-constructed using the iso-advector VOF method. This method usually referred to as *LES-SSAM* approach is used to simulate the primary atomization of ECN Spray-A. While in comparison to the *standard LES* approach without any SGS models, the *LES-SSAM* seems to provide relatively large number of small ligaments sheared from jet surface, this is not well reflected in the first-order statistics of liquid-volume fraction. Therefore, a further assessment in terms of resulting droplet size statistics is necessary to evaluate the performance of the *LES-SSAM* approach.

Acknowledgments

The authors would like to thank the Association Nationale de la Recherche et de la Technologie (ANRT) and the Volvo group for sponsoring the project. All the simulations in this study are performed on PSMN cluster from Ecole Normale Superior, Lyon.

References

[1] Wu, P.K., Miranda, R.F. and Faeth, G.M., 1995. Effects of initial flow conditions on primary breakup of nonturbulent and turbulent round liquid jets. *Atomization and sprays*, *5*(2).

[2] Hiroyasu, H., 1991. Break-up length of a liquid jet and internal flow in a nozzle. In *Proc. 5th. ICLASS* (pp. 275-282).

[3] Andriotis, A., Gavaises, M. and Arcoumanis, C., 2008. Vortex flow and cavitation in diesel injector nozzles. *Journal of Fluid Mechanics*, *610*, pp.195-215.

[4] Tryggvason, G., Bunner, B., Esmaeeli, A., Juric, D., Al-Rawahi, N., Tauber, W., Han, J., Nas, S. and Jan, Y.J., 2001. A front-tracking method for the computations of multiphase flow. *Journal of computational physics*, *169*(2), pp.708-759.

[5] Sussman, M., Smereka, P. and Osher, S., 1994. A level set approach for computing solutions to incompressible two-phase flow.

[6] Hirt, C.W. and Nichols, B.D., 1981. Volume of fluid (VOF) method for the dynamics of free boundaries. *Journal of computational physics*, *39*(1), pp.201-225.

[7] Chesnel, Jeremy, Thibaut Menard, Julien Reveillon, and Francois-Xavier Demoulin. "Subgrid analysis of liquid jet atomization." *Atomization and Sprays* 21, no. 1 (2011).

[8] Herrmann, M. and Gorokhovski, M., 2008. An outline of a LES subgrid model for liquid/gas phase interface dynamics. Proceedings of the 2008 CTR Summer Program, pp.171-181.

[9] Sabel'nikov V, Chtab-Desportes A, Gorokhovski M. New sub-grid stochastic acceleration model in les of high-Reynolds-number flows. Eur Phys J B. 2011;80(2):177–87.

[10] Sabelnikov, V., Barge, A. and Gorokhovski, M., 2019. Stochastic modeling of fluid acceleration on residual scales and dynamics of suspended inertial particles in turbulence. *Physical Review Fluids*, *4*(4), p.044301.

[11] Barge, A. and Gorokhovski, M.A., 2020. Acceleration of small heavy particles in homogeneous shear flow: direct numerical simulation and stochastic modelling of under-resolved intermittent turbulence. *Journal of Fluid Mechanics*, *892*.

[12] Roenby, J., Bredmose, H. and Jasak, H., 2016. IsoAdvector: Free, fast and accurate VOF on arbitrary meshes. In *The 4th OpenFOAM User Conference*.

[13] Brackbill, J.U., Kothe, D.B. and Zemach, C., 1992. A continuum method for modeling surface tension. *Journal of computational physics*, *100*(2), pp.335-354.

[14] N. Mordant, P. Metz, O. Michel, and J.-F. Pinton. Measurement of lagrangian velocity in fully developed turbulence. Phys. Rev. Lett., 87 :214501, Nov 2001.

[15] G. A. Voth, A. La Porta, A. M. Grawford, J. Alexander, and E. Bodenschatz. Measurement of particle accelerations in fully developed turbulence. Journal of Fluid Mechanics, 469 :121–160, 2002.

[16] N. Mordant, L. Leveque, and J.-F. Pinton. Experimental and numerical study of the lagrangian dynamics of high Reynolds turbulence. New Journal of Physics, 6 :116, 2004.

[17] Pope, S.B. and Chen, Y.L., 1990. The velocity-dissipation probability density function model for turbulent flows. *Physics of Fluids A: Fluid Dynamics*, *2*(8), pp.1437-1449.

[18] Vukcevic, V., Keser, R., Jasak, H., Battistoni, M., Im, H. and Roenby, J., 2019. Development of a CFD Solver for Primary Diesel Jet Atomization in FOAM-Extend (No. 2019-24-0128). SAE Technical Paper.

[19] Kastengren, A.L., Tilocco, F.Z., Powell, C.F., Manin, J., Pickett, L.M., Payri, R. and Bazyn, T., 2012. Engine combustion network (ECN): measurements of nozzle geometry and hydraulic behavior. *Atomization and Sprays*, *22*(12), pp.1011-1052.

[20] Kastengren, A., Tilocco, F.Z., Duke, D., Powell, C.F., Zhang, X. and Moon, S., 2014. Time-resolved X-ray radiography of sprays from engine combustion network spray a diesel injectors. *Atomization and Sprays*, *24*(3).

[21] Kastengren, A., Ilavsky, J., Viera, J.P., Payri, R., Duke, D.J., Swantek, A., Tilocco, F.Z., Sovis, N. and Powell, C.F., 2017. Measurements of droplet size in shear-driven atomization using ultra-small angle x-ray scattering. *International Journal of Multiphase Flow*, *92*, pp.131-139.